PERFORMANCE ANALYSIS OF TYPICAL AIRFOILS THROUGH NUMERICAL SIMULATION USING FLUID-STRUCTURE INTERACTION

Igor Albuquerque Maia[1]

igor.albuquerque@polo.ufsc.br

[1]Universidade Federal de Santa Catarina-UFSC, Departamento de Engenharia Mecânica. 88040-535, Pantanal, Florianópolis, SC. Brazil

Francisco Ilson da Silva Júnior[2]

[2]ilson@ufc.br

[2]Universidade Federal do Ceará, Departamento de Engenharia Mecânica. Campus do Pici - Bloco 714 - CEP 60455-760 – Fortaleza, CE, Brazil.

Abstract. *The lift and drag coefficients curves as a function of the angle of attack for typical airfoils were obtained through computer simulation of the fluid-structure interaction. The airfoil was modeled as a section of a 1m chord infinite wing, and the simulation domain was modeled as a wind tunnel with 13m length and 1m width. The finite element used was a 2-D beam element which allows rotation and linear displacement in one axis. The influence of three factors upon the results was studied: the Reynolds number, the finite element cross-section and the material elasticity modulus. Three Reynolds numbers were simulated: $Re=10^6$, $Re=3x10^6$ and $Re=10^7$. Two different cross-sections were used, as well as two material elasticity moduli. The results of the fluid-structure problem were compared with the results of the fluid problem. Therefore, one could evaluate how structure stiffness modifies the pressure field and how this phenomenon influences the lift and drag coefficients.*

Keywords: *Fluid-structure interaction, Airfoil, Lift and drag coefficients.*

1 INTRODUCTION

The use of alternative energy sources is justified due to the growth of global energy demand in recent decades, the approaching limits to conventional sources consumption and the increasing environmental concern. An example of clean and alternative source is wind energy. Therefore, large structures known as wind turbines transform wind energy into mechanical energy in order to turn a propeller system for generation of electric power.

In order to model this problem, the following methodology can be used: the fluid load is imposed directly on the wind turbine structure. This load causes a dynamic response of the structure, which changes the fluid pressure field and leads to a new excitation of the structure. The interaction between the two media continues until an equilibrium position is reached or it can lead to catastrophic ruin the structure. Therefore, the study of these phenomena requires an adequate modeling of both the fluid medium as the structure.

The fluid-structure statement for coupled vibrations problems was initially established for Zienkiewicz and Newton (1969). In this formulation, it was introduced an interface domain that combines the kinematics and momentum equilibrium equations of fluid and solid domains. The fluid loading conditions can be obtained by a CFD (Computational Fluids Dynamics) model and applied on wind turbine structural model. Fluid-structure interaction problems are particularly important in the aerodynamics and aeroelasticity researches. Even as, it is important to know the loads imposed by the wind on structures and their dynamic responses, since the performance of the turbines has an intrinsic relationship with its dynamic behavior. In this context, there are two aerodynamic variables used to design aircraft and wind turbines: the lift coefficient and the coefficient of drag. The coefficients are functions of the airfoil geometric characteristics and the Reynolds number of the flow. These quantities are chosen to operate at the point where the greatest ratio among the lift and drag coefficients.

The goal of this study is to model the fluid-structure interaction of a typical airfoil section used in the design of wind turbine blades. Therefore, this work aimed to trace the curves of lift and drag coefficients as a function of angle of attack for an airfoil S809 by two methodologies. The first one is obtained through a CFD solution for the fluid flow with a rigid structure hypothesis and another one done by a fluid-structure analysis. It was compared the curves obtained by the two methodologies. Another objective of this work is to determine the coupling among the structural stiffness and the pressure loading disturbance of the flow. A study of the influence of Reynolds number on the results was made. Moreover, it was obtained the influence of the geometrical properties of the airfoil structure on the model results. The airfoil was modeled as a beam element with constant modulus, the same as in (Puterbaugh and Beyene, 2011), except that the section of the beam was kept constant from the trailing edge to the leading edge. The material used for the beam shaping glass fiber was type E-glass, whose properties are available in The Journal of Materials AZO online (AZO, 2012). The simulations were performed with the commercial package ANSYS Mechanical, which uses the FLOTRAN solver for the fluid problem. The methodology for obtaining the lift coefficient and drag coefficient from the pressure coefficient obtained by simulation was similar to that developed by Seraphim (2004).

The outline of the rest of the paper is as follows. In Section 2, aerodynamical concepts of a Horizontal-Axis Wind Turbine are described. Moreover, the basic assumptions of the model are presented. In the next section, we state the fluid-structure problem. For the structure, Kirchoff-Love assumptions are presented by mechanical governing equations description. For the fluid domain, the Non-Linear Navier-Stokes equations are presented in fluid dynamics

section. In Section 4, the computational method is illustrated. In Section 5, the numerical results are presented and the performance of the coupled system is estimated by typical graphs. The conclusions are outlined in Section 6.

2 AERODYNAMIC CONCEPTS

Despite the complexity that a certain flow pattern may have, there are only two ways a fluid can transmit force to a body: through the pressure distribution and the shear stress distribution. The net effect of pressure and shear distributions integrated over the surface of a body is an aerodynamic force and a momentum, which are shown in Fig. 1.

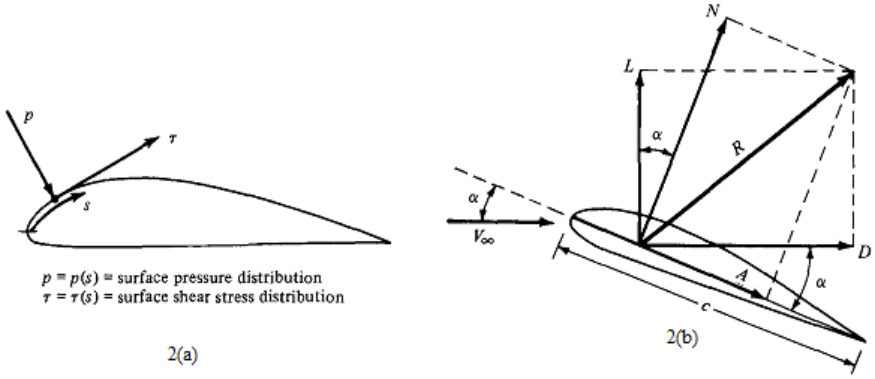

Figure 1. Forces acting on an airfoil(a); Resultant aerodynamic forces(b). (Anderson Jr., 2001)

where L and D are the lift and drag force respectively and A and N are the components of the aerodynamic force in the directions parallel and perpendicular to the airfoil chord, respectively. α is the angle of attack.

Consider now the airfoil shown in Fig. 2, which is a cross-section of wing with an infinite length. Let A and B be two arbitrary points taken in the upper and bottom surfaces, respectively. The pressure and shear in the upper surface are represented by s_u and τ_u whilst the pressure and shear at the bottom surface are represented by s_b and τ_b.

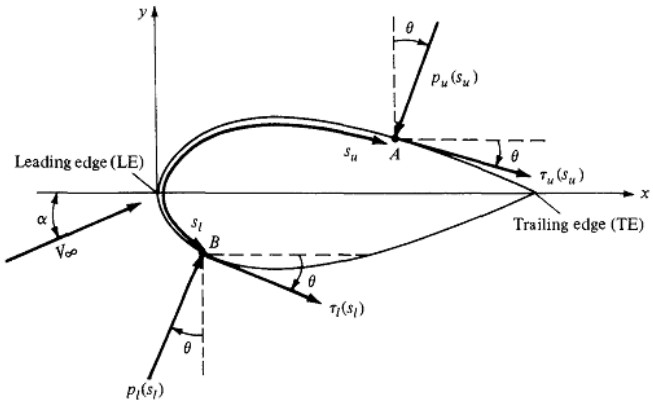

Figure 2. Nomenclature of pressure and shear distributions for integration. (Anderson Jr., 2001).

One can integrate the pressure and shear distributions over the upper and bottom surfaces, from the leading edge to the trailing edge to obtain the forces per unit length, N' and A', as follows in eq. (1) and (2):

$$N' = -\int_{LE}^{TE} \left(p_u \cos\theta + \tau_u \sin\theta \right) ds_u + \int_{LE}^{TE} \left(p_d \cos\theta - \tau_b \sin\theta \right) ds_b \tag{1}$$

$$A' = \int_{LE}^{TE} \left(-p_u \sin\theta + \tau_u \cos\theta \right) ds_u + \int_{LE}^{TE} \left(p_d \sin\theta - \tau_b \cos\theta \right) ds_b \tag{2}$$

where p_u and p_l are the pressure in the upper and lower surfaces of the airfoil; τ_u and τ_l are the shear acting on the upper and lower surfaces, respectively.

The lift and drag forces per unit span can be obtained through these two expressions, by means of the trigonometric relations between the forces and the angle of attack. These forces may be expressed in terms of dimensionless coefficients, namely, the pressure coefficient C_p and the friction coefficient C_f. They become the dimensionless coefficients c_n and c_a, stated by Eq. (3) and Eq. (4).

$$c_n = \frac{1}{c}\left[\int_0^c \left(C_{p,l} - C_{p,u} \right) dx + \int_0^c \left(C_{f,u} \frac{dy_u}{dx} - C_{f,l} \frac{dy_l}{dx} \right) dx \right] \tag{3}$$

$$c_a = \frac{1}{c}\left[\int_0^c \left(C_{p,u} \frac{dy_u}{dx} - C_{p,l} \frac{dy_l}{dx} \right) dx + \int_0^c \left(C_{f,u} + C_{f,l} \right) dx \right] \tag{4}$$

where $C_{p,u}$ and $C_{p,l}$ are the pressure coefficients on the upper and lower surfaces, respectively; $C_{f,u}$ and $C_{f,l}$ are the friction coefficients on the upper and lower surfaces, respectively and c is the chord length of the airfoil.

If one neglects the influence of viscous friction, which is a reasonable assumption for flows with high Reynolds numbers, Eq. (5) and Eq. (6) yield simplified expressions for the dimensionless coefficients c_n and c_a.

$$c_n = \frac{1}{c}\int_0^c \left(C_{p,l} - C_{p,u} \right) dx \tag{5}$$

$$c_a = \frac{1}{c}\int_0^c \left(C_{p,u} \frac{dy_u}{dx} - C_{p,l} \frac{dy_l}{dx} \right) dx \tag{6}$$

The lift and drag coefficients C_l and C_d may then be obtained by decomposing c_n and c_a in the directions parallel and perpendicular to the flow using the same trigonometric relations as those we have for the forces. Equations (7) and (8) show these expressions.

$$c_l = c_n \cos\alpha - c_a \sin\alpha \tag{7}$$

$$c_d = c_n \sin\alpha + c_a \cos\alpha \tag{8}$$

where α is the angle of attack.

3 PROBLEM DESCRIPTION

In this paper, simulations were performed considering the airfoil as a section of an infinite blade with a constant chord of 1m length. The domain used in the simulations was a wind tunnel of 1m length and 1m width. The domain was split into three parts: the first one is the region upwind of the airfoil, where the mesh is static; the second one is the region near the airfoil. In this region, the mesh was set to be dynamic, and it is where the fluid-structure interaction itself occurs, i.e., it is where the mesh will deform due to the airfoil displacement. The third region is the one downwind of the airfoil.

For the meshing process to succeed, the nodes of the finite element mesh were set to coincide with the CFD mesh nodes. The finite element mesh near the airfoil is shown in Fig. 3.

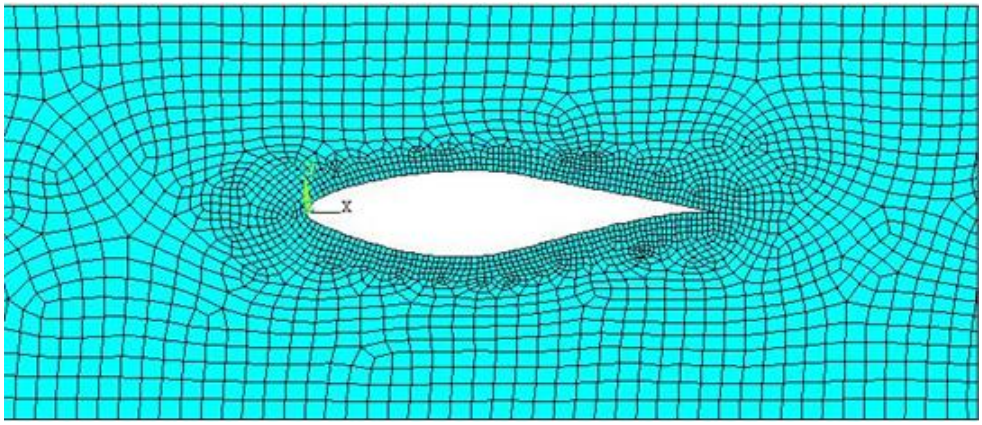

Figure 3. Finite element mesh near the airfoil

The simulations were carried out for the following values of the angle of attack: 0º, 5º, 10º, 15º, 20º, 25º and 30º. The airfoil was modeled with a beam finite element, which allows displacement in one axis and rotation over one axis. The influence of three parameters was evaluated: the Reynolds number, the geometric properties of the finite element and the material elasticity modulus. Three Reynolds numbers were simulated: Re = 10^6; Re = $3x10^6$; Re = 10^7. The influence of the geometric properties of the finite element was evaluated by reducing its cross-section. The properties are shown in Tab. 1.

Table 1- Geometric properties of the beam finite element.

	Surface (m^2)	Area Moment of Inertia (m^4)	Height (m)
Cross-Section 1	$8 \cdot 10^{-5}$	$2.667 \cdot 10^{-8}$	$2 \cdot 10^{-2}$
Cross-Section 2	$5 \cdot 10^{-5}$	$1.042 \cdot 10^{-10}$	$5 \cdot 10^{-3}$

The material used to model the airfoil was the E-glass fiber, a composite material commonly used in the manufacture of wind turbine blades. The properties of this material were obtained from (AZO, 2012). Its normalized elasticity modulus for this material is 78.5MPa. In order to verify the influence of a less stiff material, i.e., with a lower elasticity modulus,vis upon the lift and drag coefficients, the simulations were repeated for a fictitious material with an elasticity modulus of 39.25MPa, which is half of the E-glass modulus.

At the Reynolds number considered in this work, compressibility effects become important. They tend to move the aerodynamic center aft of the ¼ chord (Anderson, 2001). For this model, it was assumed that the airfoil center of pressure was located at a distance of 1/3 of the chord length from the leading edge. All the degrees of freedom were constrained at this point. The k-e turbulence model was used in this analysis.

The CFD problem was simulated separately with the same Reynolds numbers cited above, in order to compare the results obtained from the two methods.

With the ANSYS post-processing tools, it is possible to map the pressure coefficient C_p over the upper and lower surfaces of the airfoil for each simulation. The dimensionless coefficients c_n and c_a can then be obtained through Eq. (5) and Eq. (6). These coefficients are related to the lift and drag coefficients by Eq. (7) and Eq. (8). Here we neglect the influence of viscous friction on the overall forces exerted by the fluid on the airfoil to compute the coefficients, which is a reasonable assumption to high Reynolds number flows. However, the flow solver carries out the solution considering viscous effects on the wall. Using this procedure, the lift and drag coefficients were evaluated over the range of the angle of attack considered in this case.

4 COMPUTATIONAL STRATEGY

In this paper, the solution was obtained by commercial tools. The Finite Element Code ANSYS solves the integral equations for dynamic fluid conditions. In this approach, a fluid-structure interface is required to connect the fluid and solid areas and allow the deformation of the mesh. For coupled problems analysis, this interface is located on the contours common to these two areas. The central region of the diagram represents the fluid-structure interface. A diagram containing the steps of the simulation is shown in Fig. 4.

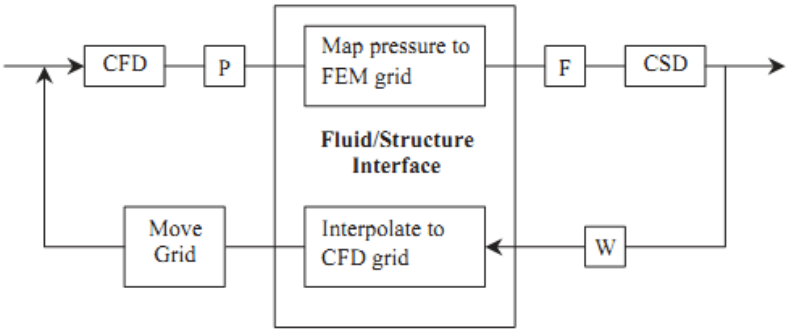

Figure 4 – Fluid-Structure Strategy. (Kamakoti and Shyy, 2004).

The analysis begins with a Fluid Analysis where the pressure field on the fluid domain is determined. The structural loading is calculate on the Fluid-Structure Interface and the forces are projected on the airfoil surface. The CSD (Computational Structural Dynamics) package calculates the displacements w and applies them in the fluid mesh, which was set with coincident nodes with the structural mesh. In the next step, the results are transferred and a mesh fluid grid interpolation is performed. The CFD (Computational Fluid Dynamics) package recalculates the domain problem with new boundary conditions settings. The pressure field P in the fluid domain is evaluated at each iteration and passed to the structural domain to obtain the forces F which are used to determine the structural vector displacements w. These values are interpolated on the mesh domain and the fluid pressure field is

recalculated. This procedure is repeated until convergence is reached. Generally, the mesh of the structural domain is coarser than the mesh of the fluid domain. In this case, interpolation schemes techniques can be used to transfer the fluid pressure loading. In the next section, a numerical analysis of a wind turbine airfoil is presented. The lift and drag coefficients were evaluated by several numerical tests.

5 RESULTS

In this section, one presents the numerical results obtained for a fluid-structure interaction analysis compared to CFD results. The numeric tests were performed by coupling the wind air that passes on the S809 airfoil surface. The influence of the Reynolds number upon the lift and drag coefficients results can be observed in Fig. 5, Fig. 6 and Fig. 7, which show the comparison of the lift and drag coefficients curves obtained by the two simulation methods, for Re=10^6, Re=3x10^6, and Re=10^7, respectively. The data obtained were fitted with a spline interpolation.

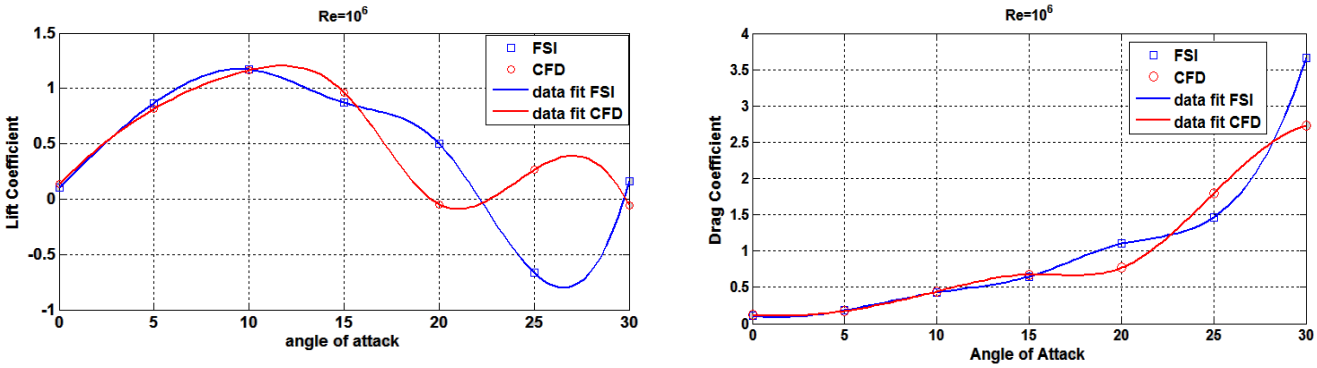

Figure 5. Lift and Drag Coefficient curves vs. angle of attack for Re= 10^6.

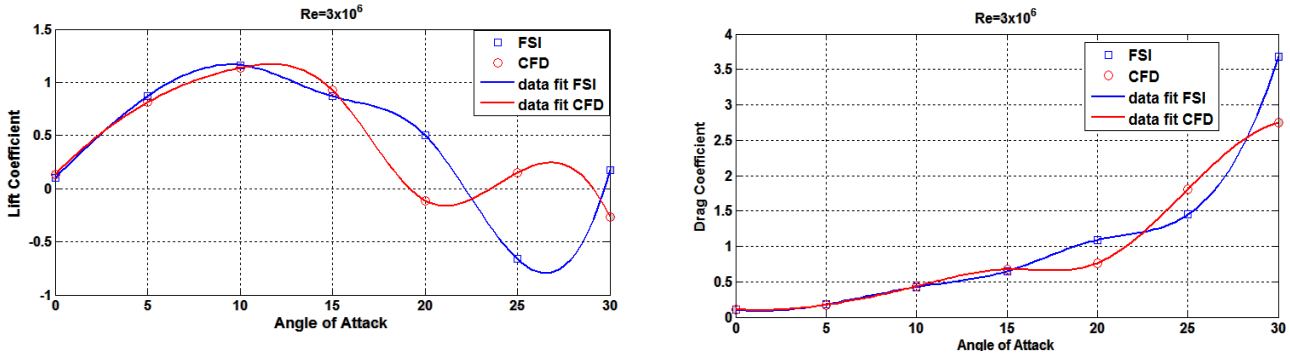

Figure 6. Lift and Drag Coefficient curves vs. angle of attack for Re= 3x10^6.

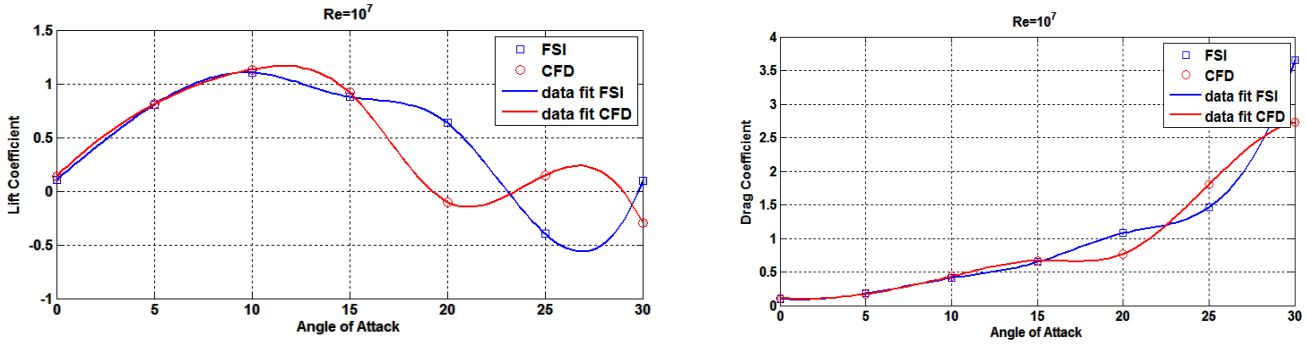

Figure 7. Lift and Drag coefficient curves vs. angle for Re= 10^7.

One can verify through the curves that the Reynolds number did not present significant influence upon the coefficients. The curves of the two methods present a good agreement until the angle of stall, which is approximately 12º, especially for $Re=10^7$, under which the results have shown the least discrepancy. However, when one takes into account the fluid-structure interaction, the stall occurs at smaller angles of attack. After the stall, the curves of the two coefficients presented significant divergence for the three Reynolds numbers simulated. The values of the drag coefficients obtained through the CFD problem were largely overestimated compared to experimental data found in literature, especially after the stall (Somers, 1997). This is due to difficulties on the solution of the turbulence model under the condition of displacement of the boundary layer (Fernandes et al., 2009).

Figure 8 shows the results for the finite element with the reduced cross-section, named cross-section 2 in Tab.1. The simulations were performed with a Reynolds number $Re=10^7$.

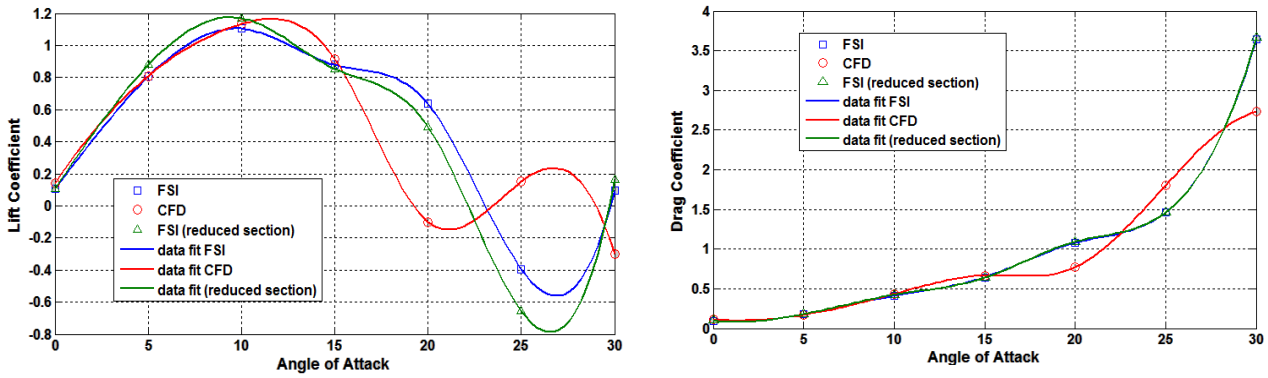

Figure 8. Influence of the beam element cross section on the lift and drag coefficients

It may be observed on the curves that with the reduction of the cross-section, the lift coefficient values became higher before the stall. Nevertheless, after the stall, a great divergence between the two methods still exists. The drag coefficient behavior, on the other hand, did not suffer the influence of the cross section reduction. Its values for the FSI problem were close to those of the CFD problem. Figure 9 shows the influence of material elasticity on the coefficients. The simulations were carried out using $Re=10^7$ for a fictitious material which has an elasticity modulus equal to half of the one used before.

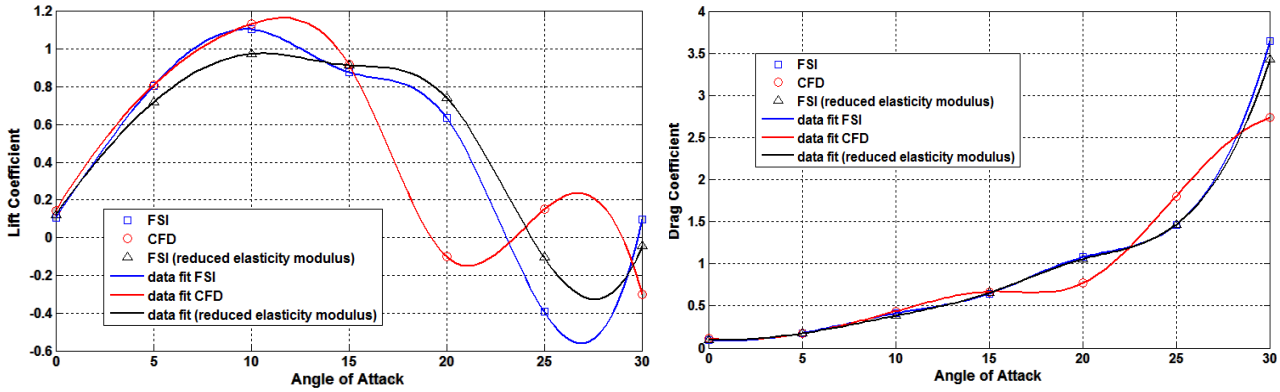

Figure 9. Influence of material elasticity modulus on the lift and drag coefficients.

One can verify that by reducing the elasticity modulus of the, the lift coefficient are also reduced and consequently the error between the two methods increases. It can also be verified that material elasticity has caused greater influence than the element cross section.

The reduced elasticity modulus has also provided a less abrupt drop lift after the stall. However, the differences between the methods remained large after this point. The drag coefficient was not affected by the reduction on the elasticity modulus. 10^7

6 CONCLUSIONS

In this paper, the lift and drag coefficient curves were obtained for an S809 airfoil through computer simulation of the fluid structure interaction. The airfoil was modeled with a 2D beam finite element. The results of the fluid structure simulation were compared with the results from a CFD analysis of the same case. The influence of three parameters upon the results was evaluated: the Reynolds number, the cross-section of the finite element and the elasticity modulus of the material.

The Reynolds number has not exerted significant influence over the lift and drag coefficients. The behavior of the curves was similar for the three Reynolds numbers simulated: before the stall, the results of the fluid structure interaction and the CFD problem have shown good agreement, although the FSI solution shows that by taking into account the influence of the displacements in the pressure and velocity fields, the stall was postponed. However, after the stall, it was found that the curves to diverge significantly, due to difficulties on the solution of the turbulence model under the condition of displacement of the boundary layer. The reduction on the element cross-section resulted in higher values of the lift coefficient in comparison with the CFD results and exerted a greater influence compared to the Reynolds number. The drag coefficient was not affected by the reduced cross-section. The material elasticity modulus has shown the greatest influence over the lift coefficient. The reduction of the elasticity modulus yielded a reduction on the lift coefficient more significant than that provided by the reduction of the cross-section and the Reynolds number. The less stiff material has also provided a smother drop of the lift coefficient after the stall. The drag coefficient, on the other hand, did not suffer any influence of this parameter either.

The two simulation approaches were found to provide similar behaviors for the coefficients from the 0º angle of attack until the stall angle, which for the S809 airfoil was approximately 12º. After this point, the results presented a high divergence for the parameters analyzed. After the stall, the behavior of the flow is governed by unsteady non-linear phenomena, and therefore, there is great difficulty in solving this kind of problem with the k-e turbulence model. Hence, the results in this part of the curves are strongly affected by this drawback. However, the behavior of the lift and drag curves until the stall angle was well captured, and is in agreement with classical results found in the literature. Therefore, the fluid-structure approach is valid as a means to gain insight about material and structural properties that may influence aerodynamic performance.

ACKNOWLEDGEMENTS

The authors would like to thank CNPq (Conselho Nacional de Pesquisa) and Capes (Coordenação de Aperfeiçoamento de Pessoal de Nível Superior) for financial support for this work.

REFERENCES

Anderson Jr., J.D., 2001. *Fundamentals of aerodynamics***.** 3rd. Ed. New York: McGraw Hill, 892p.

AZO, 2012. "The AZO journal of materials online". 1 Oct. 2012 <http://www.azom.com/properties.aspx?ID=764>.

Fernandes, M. P. G., Rocha, P. A. C., Modolo, A. B., Carneiro, F. O. M., 2009. "Estudo da convergência de malha na solução numérica de escoamento sobre perfil aerodinâmico utilizando o Open FOAM". In: *CONGRESSO BRASILEIRO DE ENSINO DE ENGENHARIA*, p-37, 2009, Recife. Anais. Recife: Poli/UPE.

Kamakoti, R.; Shyy, W., 2004. "Fluid-structure interaction for aeroelastic applications". Progress in aerospace sciences, n.40, p.535-558.

Puterbaugh, M.; Beyene, A., 2011. "Parametric dependence of a morphing wind turbine blade on material elasticity". *Energy*, n.36, p.466-474.

Seraphim, R. M., 2004. *Avaliação experimental e computacional dos coeficientes de arraste e sustentação de um aerofólio*", 25f. Monografia (Graduação em Engenharia Mecânica Automação e Sistemas) – Universidade de São Francisco, São Paulo, Itatiba.

Somers, D. M., 2012. "Design and experimental results for the S809 airfoil". Pennsylvania: National Renewable Energy Laboratory, 1997. 104p. 1 Nov. 2012 <http://www.osti.gov/bridge/product.biblio.jpg?osti_id=437668>.

Zienkiewicz, O.C. and Newton, E., 1969. "Coupled vibrations of a compressible fluid". In *Proceedings of International Symposium on Finite Elements Techniques*. pp. 359–379.